Hybrid Eulerian and Lagrangian Simulation of Steep and Breaking Waves and Surface Fluxes in High Winds

Lian Shen
Department of Civil Engineering
Johns Hopkins University
Baltimore, MD 21218
phone: (410) 516-5033 fax: (410) 516-7473 email: LianShen@jhu.edu

Robert A. Dalrymple
Department of Civil Engineering
Johns Hopkins University
Baltimore, MD 21218
phone: (410) 516-7923 fax: (410) 516-7473 email: rad@jhu.edu

LONG-TERM GOALS

This research aims at developing a numerical capability using a Lagrangian Smoothed Particle Hydrodynamics (SPH) method and an Eulerian Level-Set Method (LSM) for the simulation of steep and breaking waves in high winds. The ultimate goal is to establish an advanced computational framework for the investigation of wind-wave breaking in air-sea interaction processes, including the airflow separation over steep and breaking waves, the wind–wave momentum and energy transfer, the momentum and energy injection from breaking waves to the upper ocean, and the turbulence transport process.

OBJECTIVES

The scientific and technical objectives of this research are:

(1) Develop an Eulerian and Lagrangian multi-fluids simulation capability by using the SPH and LSM with environmental input provided by coupled wind and wave simulations at far field;

(2) Use the numerical method developed in (1) to simulate wind–wave–ocean interactions at small scales to elucidate flow structure;

(3) Quantify and characterize wind–wave momentum and energy transfer and the injection to the upper ocean by breaking waves; and

(4) Simulate and identify key process in turbulence transport near steep and breaking waves.

Report Documentation Page		*Form Approved* *OMB No. 0704-0188*
Public reporting burden for the collection of information is estimated to average 1 hour per response, including the time for reviewing instructions, searching existing data sources, gathering and maintaining the data needed, and completing and reviewing the collection of information. Send comments regarding this burden estimate or any other aspect of this collection of information, including suggestions for reducing this burden, to Washington Headquarters Services, Directorate for Information Operations and Reports, 1215 Jefferson Davis Highway, Suite 1204, Arlington VA 22202-4302. Respondents should be aware that notwithstanding any other provision of law, no person shall be subject to a penalty for failing to comply with a collection of information if it does not display a currently valid OMB control number.		

1. REPORT DATE **30 SEP 2012**	2. REPORT TYPE	3. DATES COVERED **00-00-2012 to 00-00-2012**
4. TITLE AND SUBTITLE **Hybrid Eulerian and Lagrangian Simulation of Steep and Breaking Waves and Surface Fluxes in High Winds**		5a. CONTRACT NUMBER
		5b. GRANT NUMBER
		5c. PROGRAM ELEMENT NUMBER
6. AUTHOR(S)		5d. PROJECT NUMBER
		5e. TASK NUMBER
		5f. WORK UNIT NUMBER
7. PERFORMING ORGANIZATION NAME(S) AND ADDRESS(ES) **Johns Hopkins University,Department of Civil Engineering,Baltimore,MD,21218**		8. PERFORMING ORGANIZATION REPORT NUMBER
9. SPONSORING/MONITORING AGENCY NAME(S) AND ADDRESS(ES)		10. SPONSOR/MONITOR'S ACRONYM(S)
		11. SPONSOR/MONITOR'S REPORT NUMBER(S)
12. DISTRIBUTION/AVAILABILITY STATEMENT **Approved for public release; distribution unlimited**		
13. SUPPLEMENTARY NOTES		
14. ABSTRACT		
15. SUBJECT TERMS		

16. SECURITY CLASSIFICATION OF:			17. LIMITATION OF ABSTRACT	18. NUMBER OF PAGES	19a. NAME OF RESPONSIBLE PERSON
a. REPORT **unclassified**	b. ABSTRACT **unclassified**	c. THIS PAGE **unclassified**	**Same as Report (SAR)**	**10**	

Standard Form 298 (Rev. 8-98)
Prescribed by ANSI Std Z39-18

APPROACH

This research builds on a hybrid simulation approach that couples several Eulerian and Lagrangian methods for free-surface turbulence and wave simulation. In the far field, coupled wind and wave simulations are used to obtain wind turbulence and wavefield, with the phases of nonlinear waves resolved, to provide realistic environmental input for the simulation of breaking waves. Specifically, LES of air turbulence is performed by using a hybrid pseudo-spectral and finite-difference method on a boundary fitted grid that follows the ocean wave surface; a high-order spectral (HOS) method is used to capture all of the dynamically important nonlinear wave interactions in the wavefield; and the wind and wave simulations are dynamically coupled through a fractional step method with two-way feedbacks.

As a wave becomes steep, LSM in a subdomain that contains the steep/breaking wave is performed to better resolve the flow field. LSM uses a signed distance function, namely the level-set function, to represent the interface implicitly. The location where the level-set function has zero value denotes the air–water interface. In the simulation, air and water together are treated as a fluid system with varying density and viscosity. In LSM, the level-set function is advected by the flow subject to a Lagrangian-invariant transport equation. To preserve the distance-function property for the level-set function, re-initialization is performed during the simulation using a sub-cell fix method. A Coupled Level-Set Volume-of-Fluid (CLSVOF) method is employed to conserve the mass precisely.

When the wave breaks, the flow at the free surface may become very violent, air and water may be highly mixed, and drops and bubbles may be formed. To better resolve the detailed structures and to robustly capture the violent flow, the SPH method is used, which is ideal for the wave breaking problem as the motion of nodal points (i.e., smoothed particles) is tracked in a Lagrangian manner.

All the codes are parallelized using message passing interface (MPI) based on domain decomposition. For SPH, graphics processing unit (GPU) computing, which is highly efficient for particle methods, is used to speed up the simulation.

WORK COMPLETED

In FY2012, substantial advancements have been made for the study of the physics of high wind over breaking waves. Good results have been obtained in the simulations and analysis of steep and breaking waves under wind forcing, which include:

- Simulation of wind turbulence over breaking water waves, with identification of breaking stages and analysis of near surface enhancement of turbulence intensity by breaking.
- Analysis of wind profile over steep and breaking waves, with quantification of friction velocity, drag coefficient, and roughness length scale.
- Analysis of wind pressure over steep and breaking waves, with quantification of form drag and drag saturation.
- Simulation of strong plunging breaker, with illustration of the formation of large scale vortices.
- Simulation of wave field generation by wind, with identification of different growth stages and analysis of wave spectra.

RESULTS

During this reporting period, further progresses have been made towards the simulation and understanding of the physics of the interaction between wind and breaking waves. Many encouraging results have been obtained. For example, wind turbulence over a breaking wave has been simulated using large-eddy simulation. In figure 1, instantaneous airside streamwise velocity contours on two vertical cuts and the water surface during the breaking process are plotted. Four breaking phases are identified: (1) the steepening-crest phase (figure 1(a, b)), when the front face of wave becomes steeper and concaved, and eventually becomes vertical; (2) the plunging-jet phase (figure 1(c, d)), when a small jet is formed and plunges toward the front surface; (3) the splashing-ploughing phase (figure 1(e-g)), when the jet plunges into water and generates splash-up, and then it ploughs on the water surface for several times and a highly turbulent surface region is generated; and (4) the decaying-scar phase (figure 1(h)), when the ploughing motion stops and underwater turbulence interacts with free surface and dissipates its energy. The breaking also enhances turbulence mixing near the surface.

In figure 2, the spanwise-averaged wave profiles at the time near and shortly after the breaking are plotted together with the experiment results of Caulliez (2002). The wave profiles from our simulation collapse very well with the reported measurement data. The asymmetrical wave crest has a steep wave front with the incline angle larger than 30° and a mild rear face with the incline angle around 15°. The profile shortly after the breaking shows good match with the near-breaking profile on the windward.

Surface roughness is an important parameter in modeling air-sea interaction, and it can be strongly affected by the wave field. The roughness length scales normalized by wave height are plotted in figure 3 together with Jones & Toba (1995)'s data and their conservative expression. The wave age in our simulation is at the edge of the reported data set. If we extend Jones & Toba's data further into the younger wave age, they are consistent with the present simulation.

Spanwise-averaged dynamic pressure in the wind after the wave breaking is plotted in figure 4. The pressure maximum goes across the wave crest and is located just above the jet. This pressure distribution is very different from the pressure distribution observed over non-breaking waves. It is induced by the local increase of surface velocity near the breaking crest. The "cat's eye" formed by the streamlines is pushed downwind by the sweeping jet, and the tip of the jet forms the critical point for air-flow separation. A strong counter-clockwise vortex is observed just above the sweeping jet, which is another evidence of the flow separation. This can also be the reason for the drag decrease after breaking.

In figure 5, the spanwise-averaged velocity field under water for a strong plunging breaker is plotted. At t=1.33T in the simulation, no strong vortical motion is observed. At t=1.78T, strong clockwisely-rotating vortical structures are formed. At t=2.22T, small co-rotating vortices with strength weaker than that at t=1.78T are observed and their rotating centers are located deeper. At t=2.67T, co-rotating vortices under each wave coalesce into one large vortex. This large vortex is consistent with that observed by Melville (2002).

We have also performed numerical simulation of wind-wave generation. The wave surfaces at different time are plotted in figure 6(a). The evolution of the root-mean-square of surface elevation is plotted in figure 6(b). Three growth stages can be identified: the first stage is when the waves grow linearly within a short period; the second stage is when the waves grow exponentially; and the third stage is when the wave slope becomes large, the growth slows down, and the nonlinear effect becomes

significant. Surface spectra at different time are plotted in figure 6(c). Initially, large wavenumber components are dominant. Then, a peak is formed in the middle, and the peak shifts towards small wavenumber (longer waves). As time evolves, the shift of the peak slows down and the energy of the peak keeps increasing. Such dynamical computation of wind and wave coupling will enable us to set up simulations much more realistic than the simulations in the literature, which will be invaluable for the investigation of wind-wave interaction dynamics.

IMPACT/APPLICATION

This project aims at developing an advanced simulation tool for multi-fluids free-surface flows that can be used to study the fundamental physics of wave breaking. The research will improve the understanding of air-sea interaction dynamics. The numerical developments in this project are expected to substantially improve the accuracy and efficiency of breaking wave simulation, which will lead to a powerful computational capability for direct comparison of measurement and modeling.
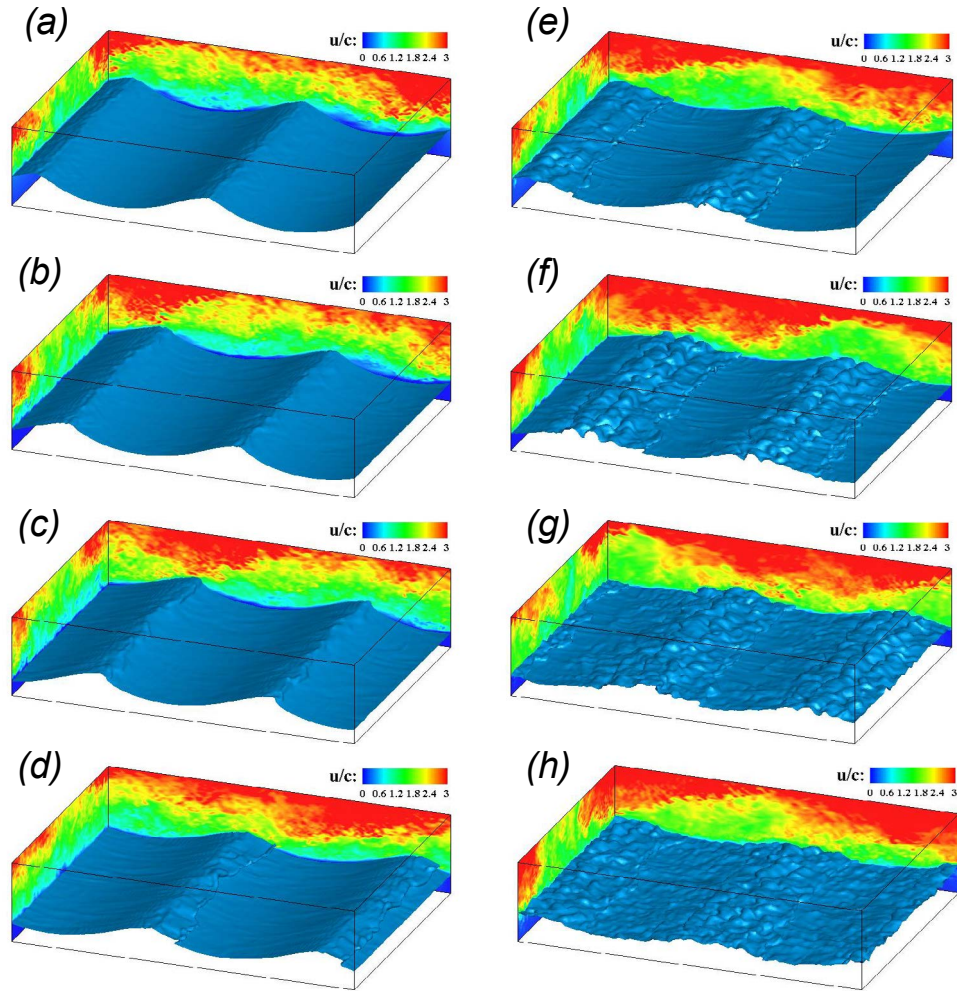
Figure 1. *Instantaneous streamwise velocity contours on two vertical cuts and the water surface of turbulent wind over a breaking Stokes wave (with wavelength 0.262m and initial wave slope* 0.35 *). The mean wind speed at 10 meter height above the mean water level is* $U_{10} = 5.06\ m/s$ *. The velocity is normalized by the dominant wave phase speed* c *.*
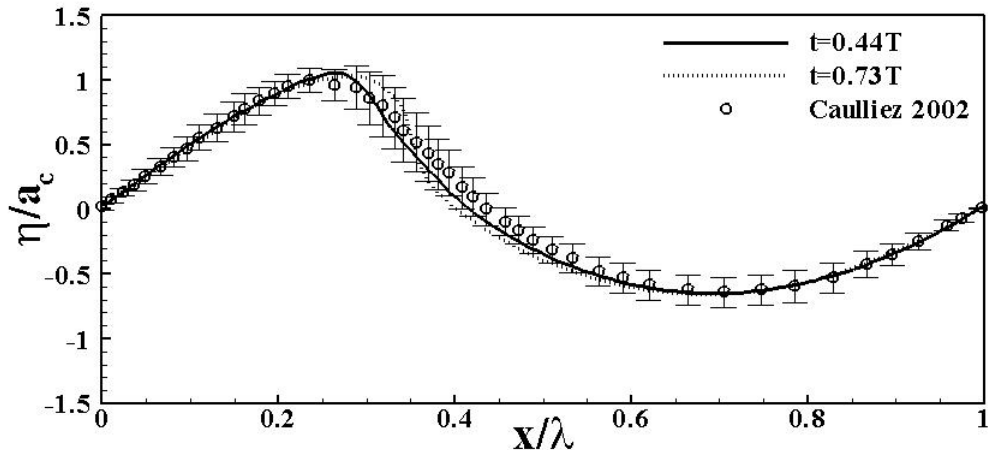
Figure 2. Spanwise-averaged wave profiles of a breaking Stokes wave with turbulent wind above (with wavelength 0.262m and initial wave slope 0.35***) near the breaking, together with Caulliez's experiment results. The mean wind speed at 10 meter height above the mean water level is*** $U_{10} = 5.06 \ m/s$***. The error bar represents the standard deviation of the measurement data.***
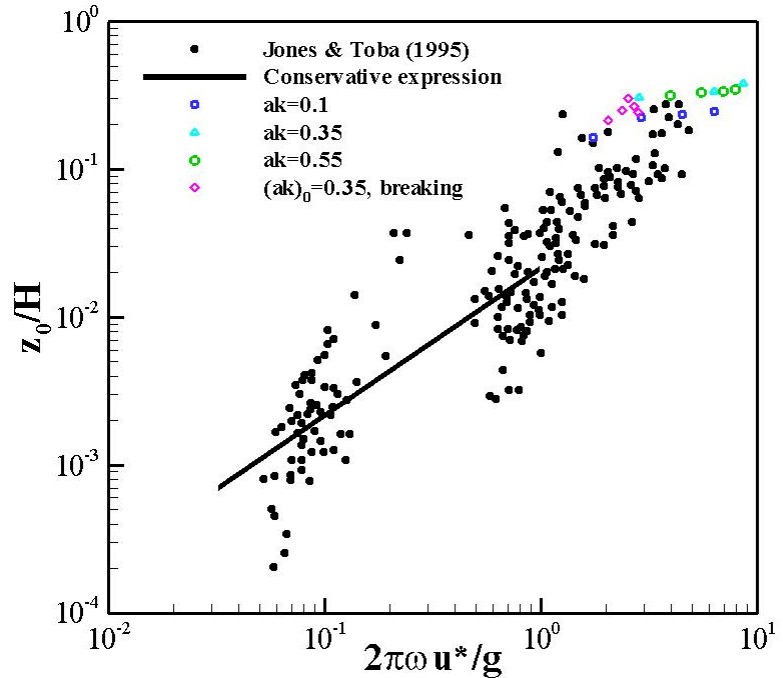
Figure 3. Roughness length scale normalized by wave height versus wave age. Stokes wave is used as the prescribed initial condition in our simulation of breaking waves. For the cases with $ak = 0.1$***, the wave length is 0.262m and the wind speeds at 10 meter height above the mean water level*** U_{10} ***are 3.91m/s, 6.35m/s, 9.72m/s, and 13.58m/s. For the cases with*** $ak = 0.35$***, the wave length is 0.262m and*** U_{10} ***are 5.06m/s, 11.08m/s, 14.97m/s, and 19.70m/s. For the cases with*** $ak = 0.55$***, the wave length is 20m and*** U_{10} ***are 22.03m/s, 30.24m/s, 37.30m/s, 42.05m/s, and 56.47m/s.***

(a)

(b)

(c)
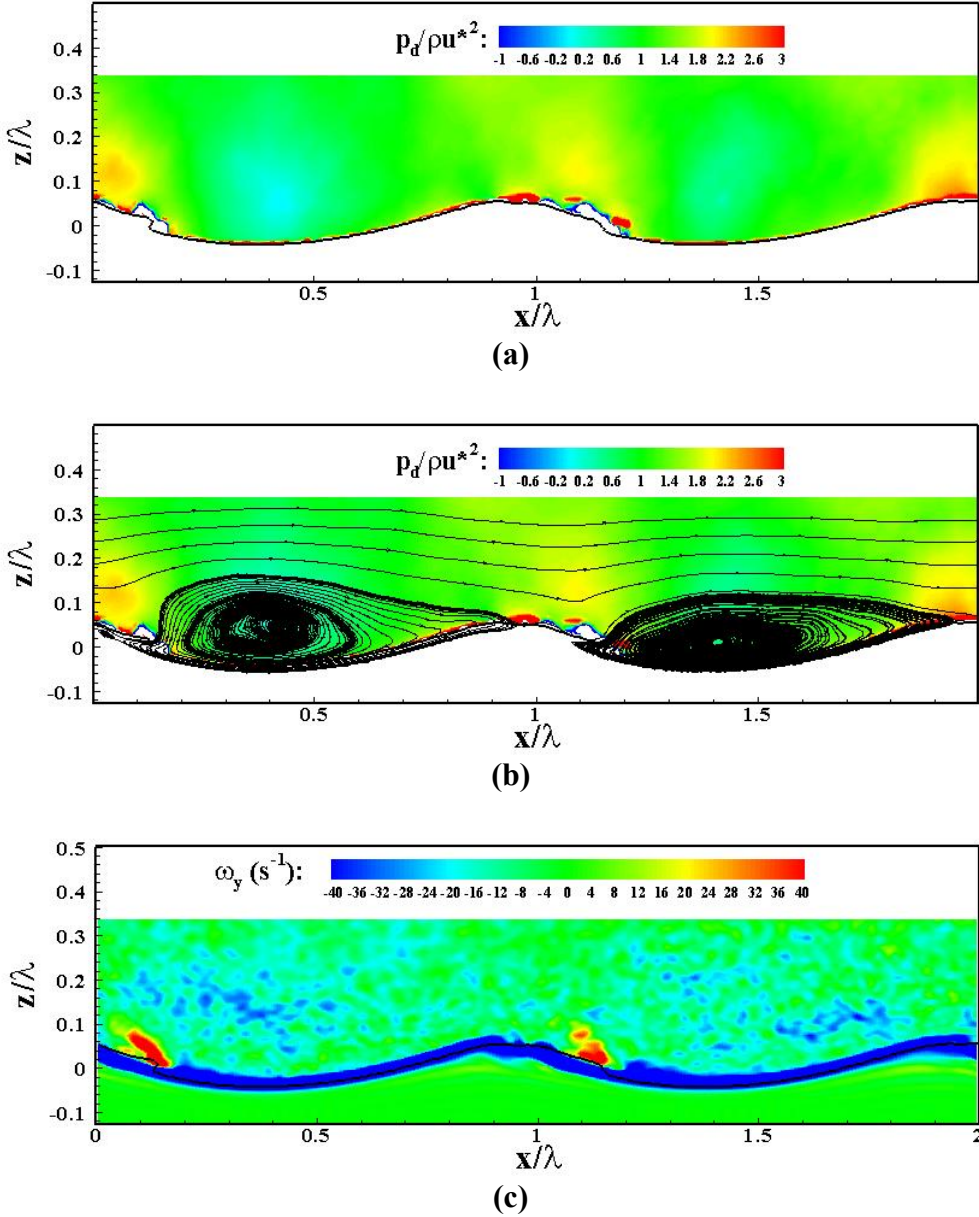
Figure 4. Spanwise-averaged dynamic pressure, streamlines, and spanwise vorticity of turbulent wind over a breaking Stokes wave (with wavelength 0.262m and initial wave slope 0.35*). The mean wind speed at 10 meter height above the mean water level is* $U_{10} = 5.06 \ m/s$*. The pressure is normalized by* $\rho u*^2$*, with* ρ *being the density of air and* $u*$ *the friction velocity of wind.*
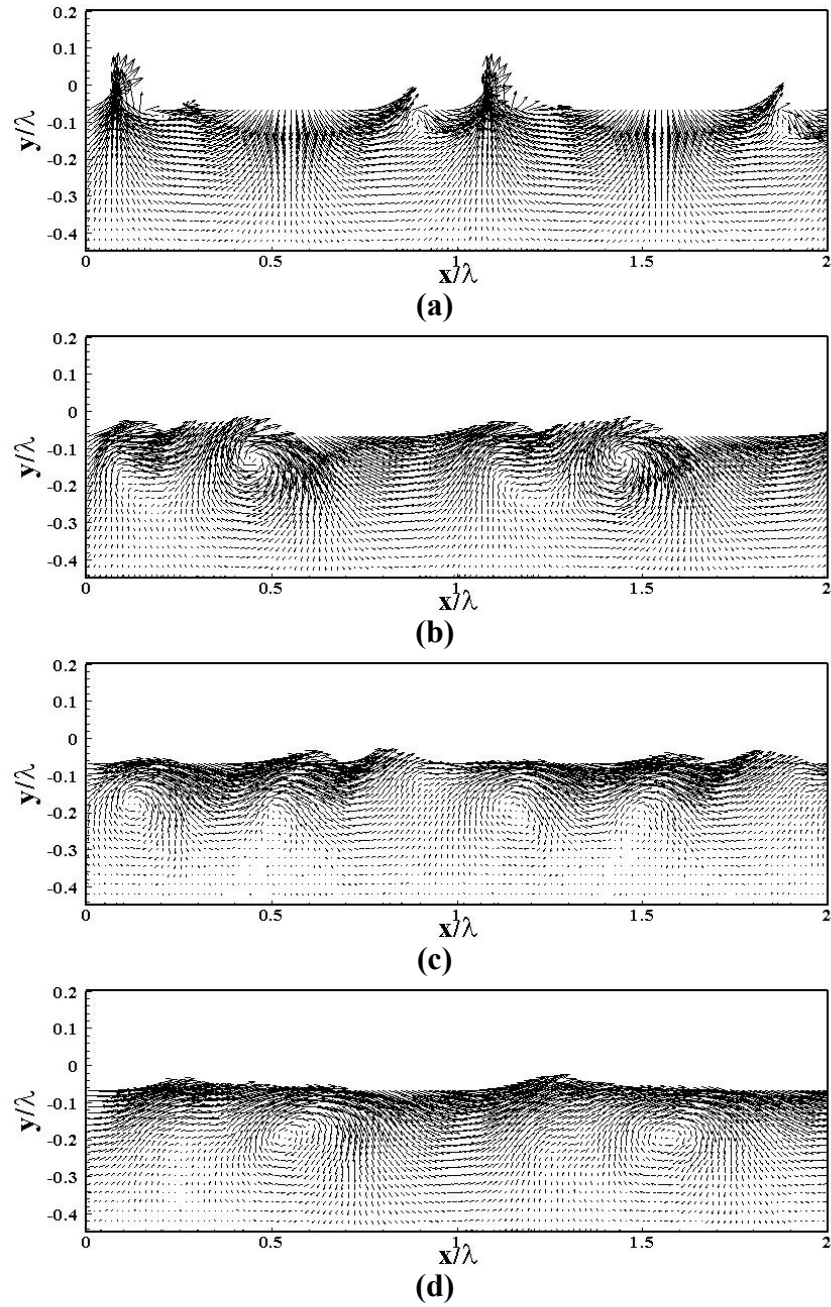
Figure 5. Instantaneous velocity vectors of spanwise-averaged water side flow field of a breaking Stokes wave (with wavelength 20m and initial wave slope 0.55*) under wind forcing at time: (a)* $t = 1.33T$ *; (b)* $t = 1.78T$ *; (c)* $t = 2.22T$ *; (d)* $t = 2.67T$ *.*
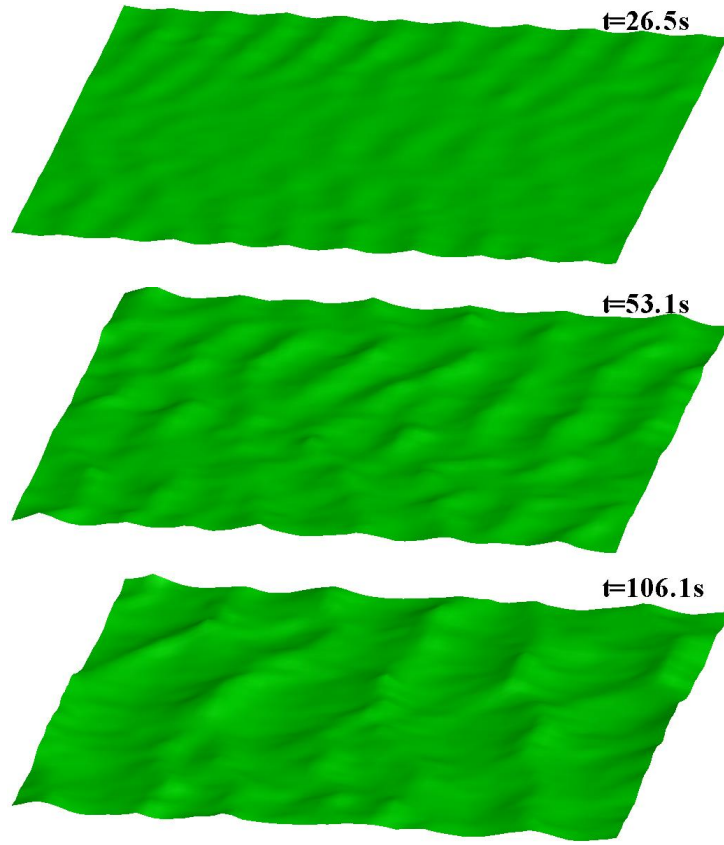
(a)
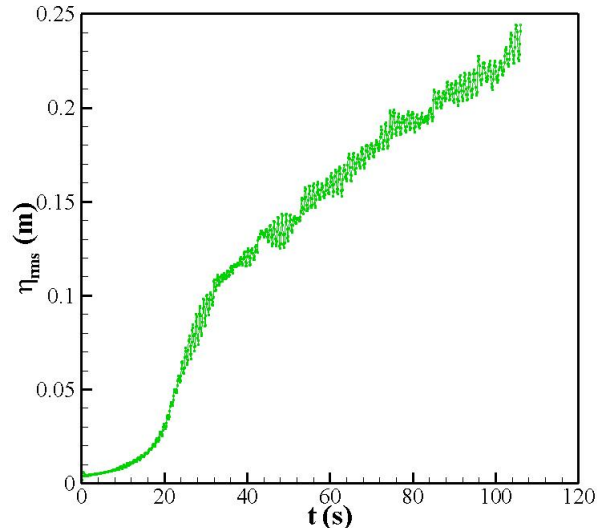
(a)
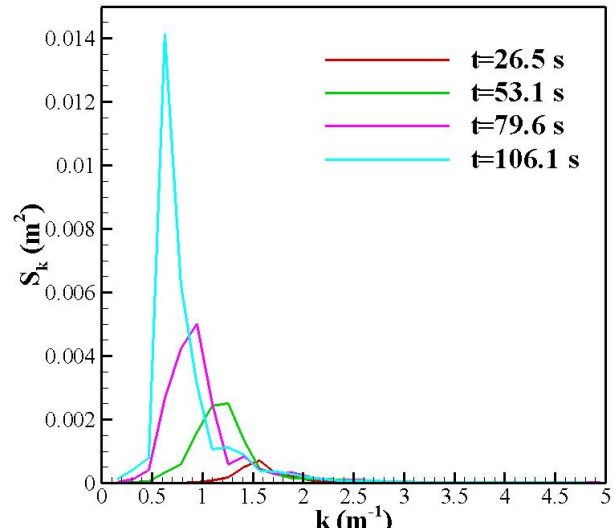
(c)

Figure 6. Waves generated by wind: (a) instantaneous wave surfaces at different time; (b) root-mean-square of surface elevation versus time; and (c) one-dimensional surface spectra of the surface elevation at different time. The mean wind speed at 10 meter height above the mean water level is $U_{10} = 30 \ m/s$.